Supplement of Earth Syst. Sci. Data, 18, 8591–8615, 2026
https://doi.org/10.5194/essd-18-8591-2026-supplement
© Author(s) 2026. CC BY 4.0 License.



Open Access Earth System Science Data

Supplement of

A multi-decadal dataset of surface damage on Antarctic ice shelves (1999–2024)

Leyue Tang et al.

Correspondence to: Gang Qiao (qiaogang@tongji.edu.cn)

The copyright of individual parts of the supplement might differ from the article licence.

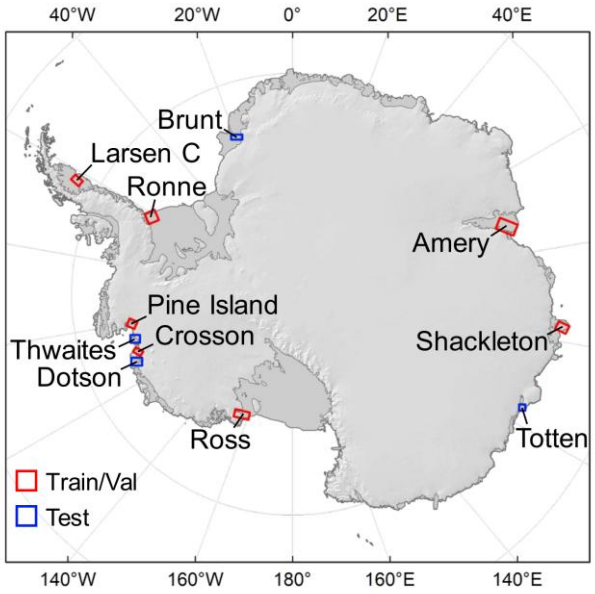


Figure S1. Spatial distribution of the source imagery used for the training/validation and test images. Red boxes indicate the regions from which the training and validation tiles were sampled, and blue boxes indicate the test regions. Training and validation tiles were split within the same ice-shelf regions. The background imagery and boundary data are from Bedmap2.

Table S1. Summary of source Landsat imagery used in the construction of the annotated surface damage dataset (for training and validation). Dates are in yyyy-mm-dd format. The spatial distribution of the selected imagery is shown in Fig. S1.

Ice Shelf	Acquisition date
Amery	2021-01-06
Crosson	2021-01-31
Larsen C	2020-12-29
Pine Island	2020-12-13
Ronne	2021-01-15
Ross	2020-12-13
Shackleton	2021-01-11

Table S2. Performance of different segmentation models on the validation set.

Model	Configuration	mIoU	OA	Precision	Recall	F1
SegFormer	B2	0.845	0.984	0.816	0.841	0.829
U-Net	ResNet-34 encoder	0.843	0.983	0.814	0.838	0.825
DeepLabV3+	ResNet-50 encoder	0.834	0.982	0.797	0.832	0.814

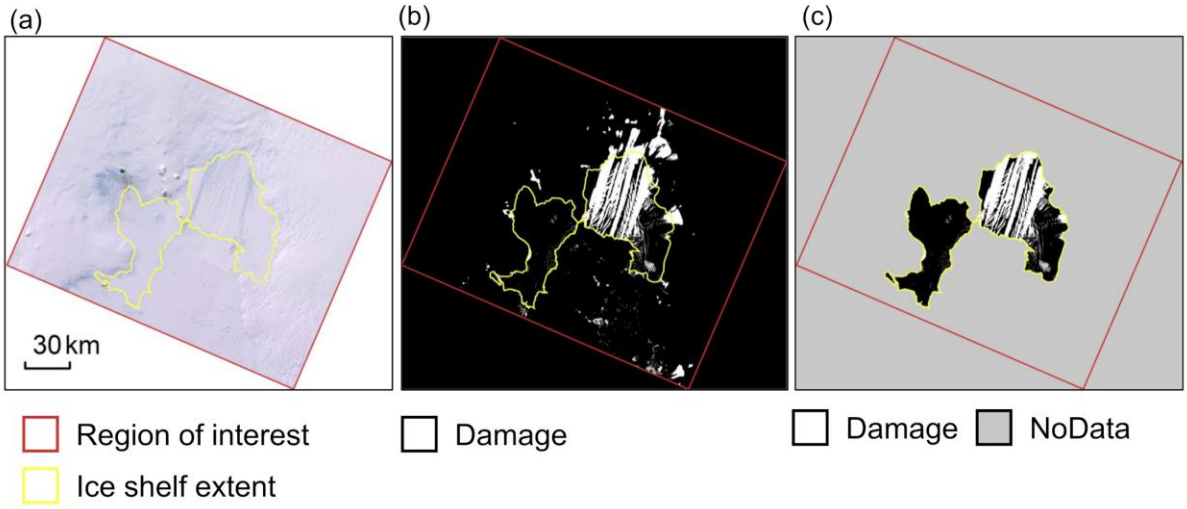


Figure S2. Illustration of the ice shelf extent constraint applied to the damage products. (a) Pine Island Ice Shelf optical image acquired in austral summer of 2021, with the red box indicating the region of interest for download and the yellow outline indicating the ice shelf extent. (b) Product type two: full-ROI damage map without spatial constraint. (c) Product type one: damage map refined by applying the ice shelf extent as a valid-domain mask, with grey areas indicating NoData regions outside the ice shelf extent.

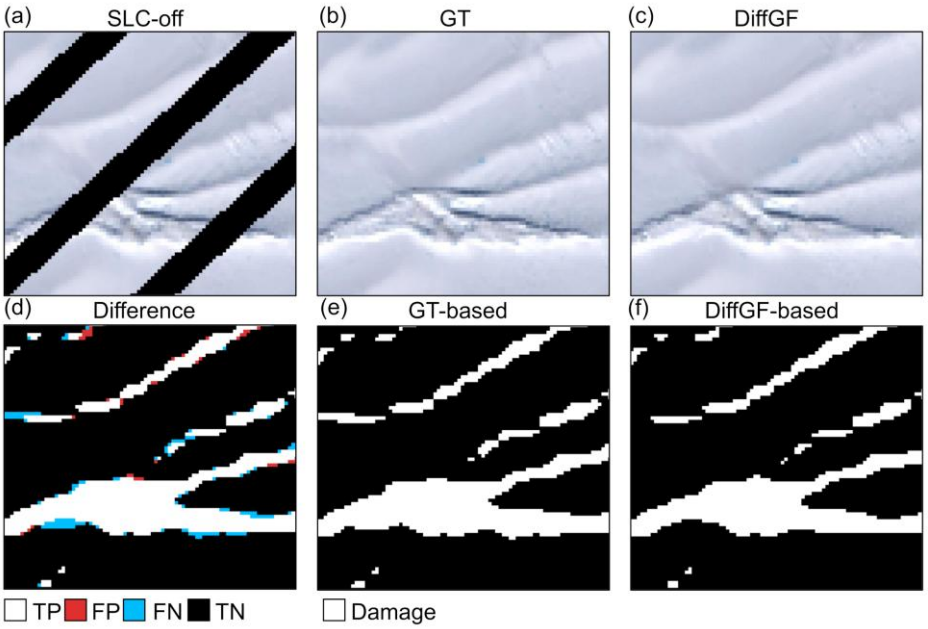


Figure S3. Red-boxed region in Fig. 11. (a) Simulated SLC-off image. (b) GT image. (c) DiffGF-restored image. (d) Pixel-wise difference map between (e) and (f), where TP denotes true positive, FP denotes false positive, FN denotes false negative and TN denotes true negative. (e) Damage segmentation derived from GT. (f) Damage segmentation derived from DiffGF restoration.

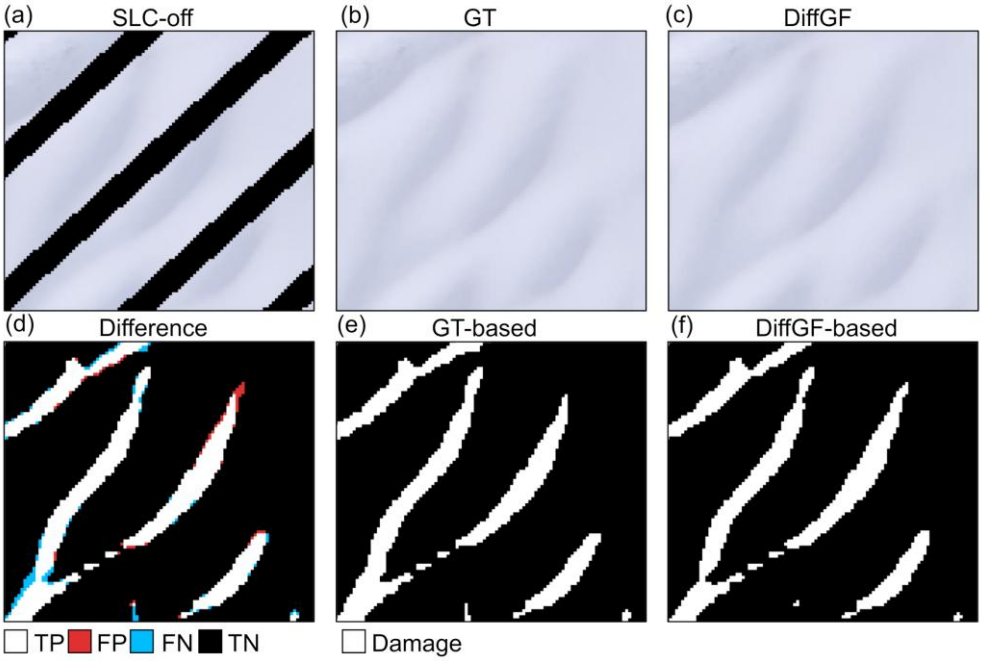


Figure S4. Yellow-boxed region in Fig. 11. (a) Simulated SLC-off image. (b) GT image. (c) DiffGF-restored image. (d) Pixel-wise difference map between (e) and (f), where TP denotes true positive, FP denotes false positive, FN denotes false negative and TN denotes true negative. (e) Damage segmentation derived from GT. (f) Damage segmentation derived from DiffGF restoration.

Table S3. Segmentation evaluation of the additional regional restoration tests against the original complete image.

Site	mIoU	OA	Precision	Recall	F1
Amery Ice Shelf	0.958	0.995	0.961	0.958	0.960
Crosson Ice Shelf	0.963	0.992	0.973	0.960	0.966
Pine Island Ice Shelf	0.956	0.978	0.986	0.962	0.974

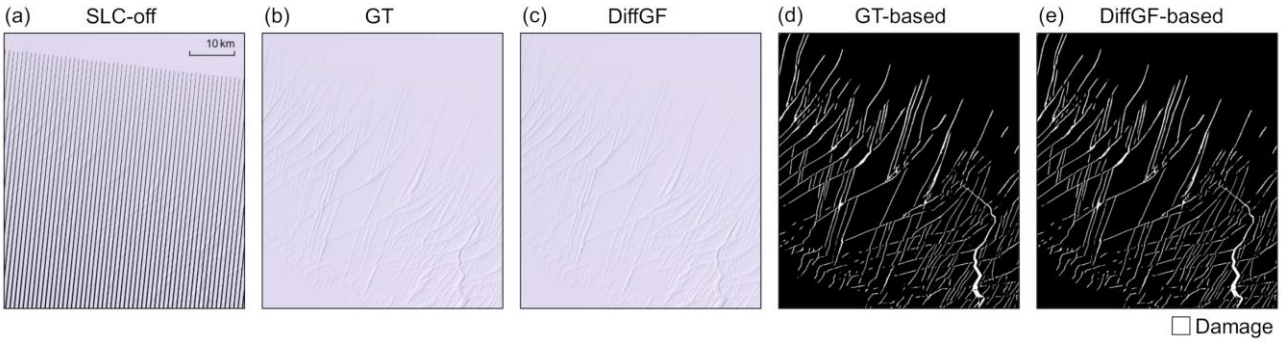


Figure S5. SLC-off restoration performance for a regional test image from Amery Ice Shelf. (a) Simulated SLC-off image generated by applying an SLC-off mask extracted from Landsat 7 imagery (2009-01-20) to Landsat 8 imagery (2016-11-15). (b) Ground truth (GT) image. (c) DiffGF-restored image. (d) Damage segmentation derived from GT. (e) Damage segmentation derived from DiffGF restoration.

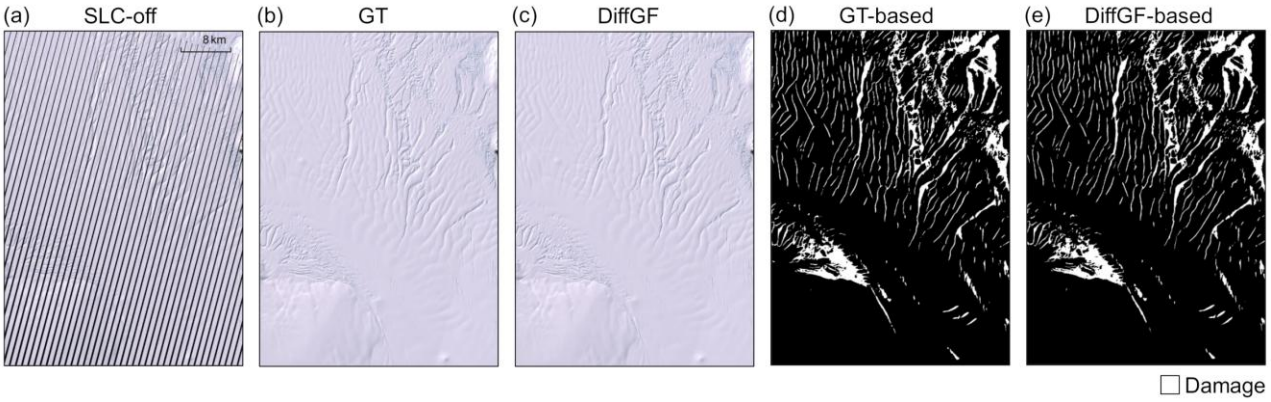


Figure S6. SLC-off restoration performance for a regional test image from Crosson Ice Shelf. (a) Simulated SLC-off image generated by applying an SLC-off mask extracted from Landsat 7 imagery (2008-02-21) to Landsat 8 imagery (2014-12-05). (b) Ground truth (GT) image. (c) DiffGF-restored image. (d) Damage segmentation derived from GT. (e) Damage segmentation derived from DiffGF restoration.

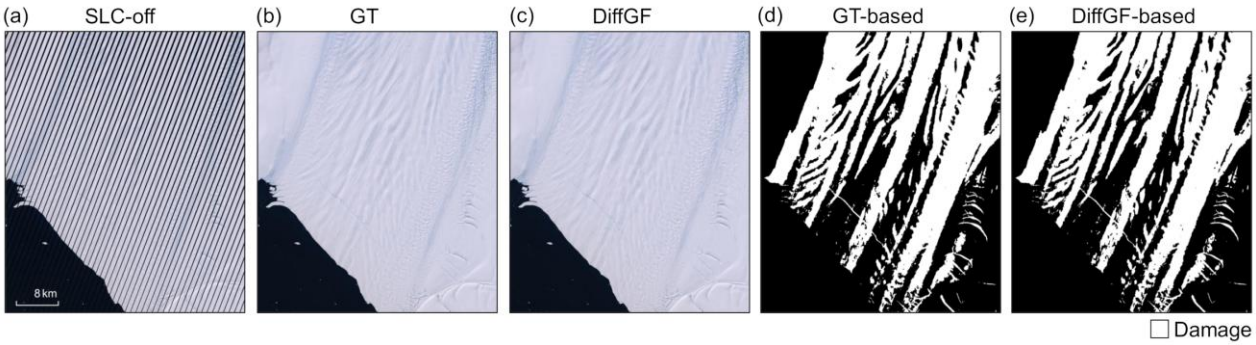


Figure S7. SLC-off restoration performance for a regional test image from Pine Island Ice Shelf. (a) Simulated SLC-off image generated by applying an SLC-off mask extracted from Landsat 7 imagery (2007-01-05) to Landsat 8 imagery (2017-01-08). (b) Ground truth (GT) image. (c) DiffGF-restored image. (d) Damage segmentation derived from GT. (e) Damage segmentation derived from DiffGF restoration.

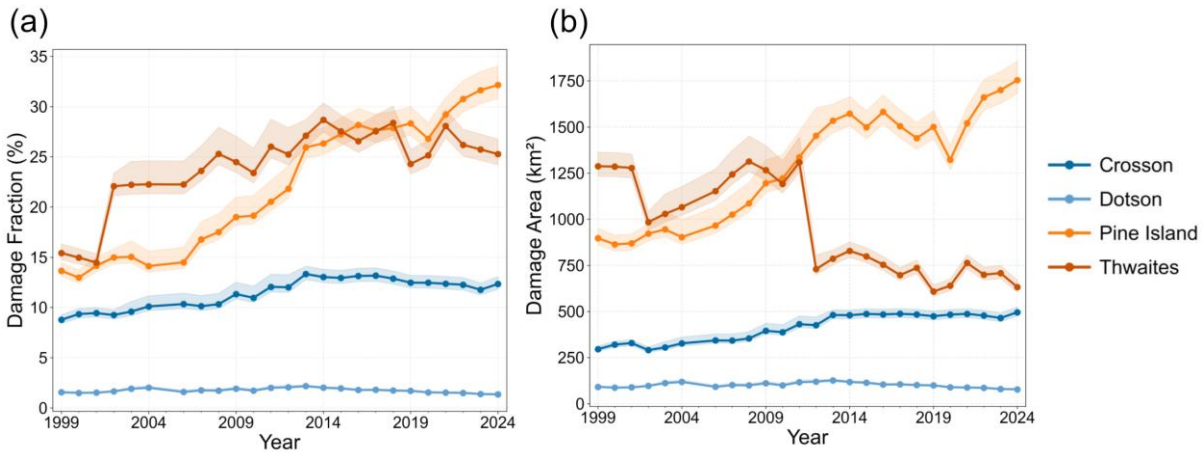


Figure S8. Temporal variations in damage fraction (a) and damage area (b) for Crosson, Dotson, Pine Island and Thwaites Ice Shelves during 1999–2024.

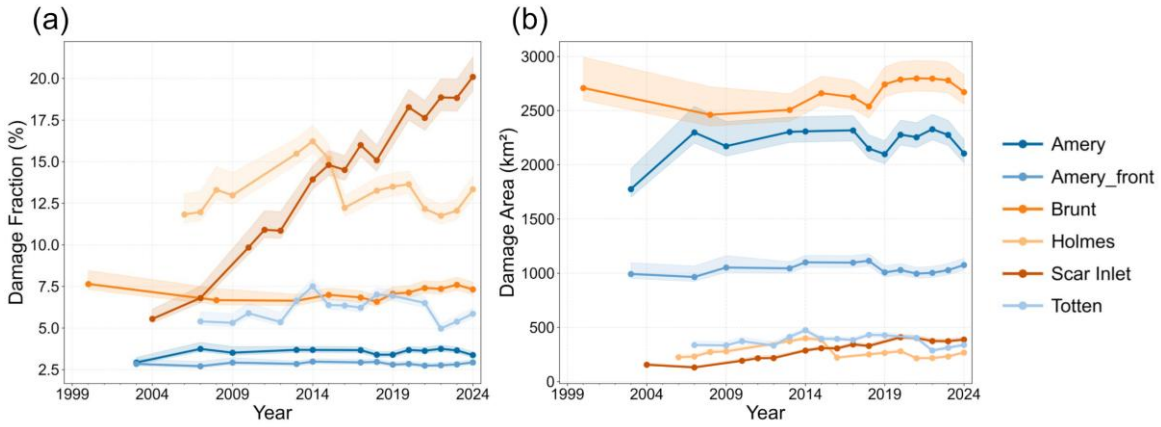


Figure S9. Temporal variations in damage fraction (a) and damage area (b) for Amery, Amery_front, Brunt, Holmes, Scar Inlet and Totten Ice Shelves during 1999–2024.

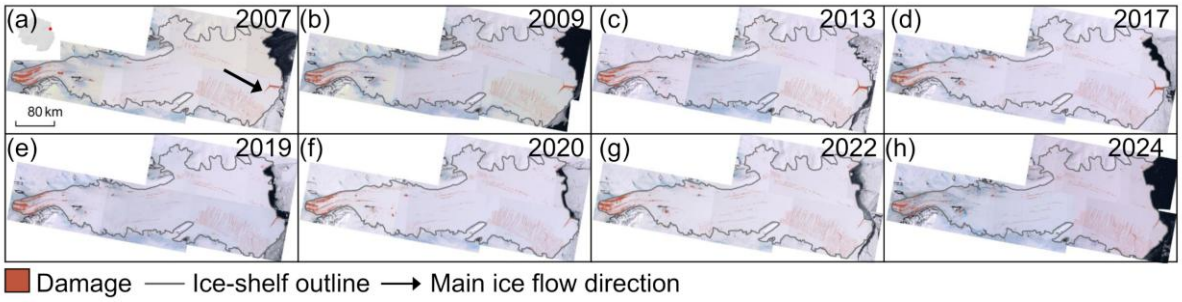


Figure S10. Representative surface damage maps of Amery Ice Shelf for (a) 2007, (b) 2009, (c) 2013, (d) 2017, (e) 2019, (f) 2020, (g) 2022 and (h) 2024. The location of Amery Ice Shelf in Antarctica is shown in (a).

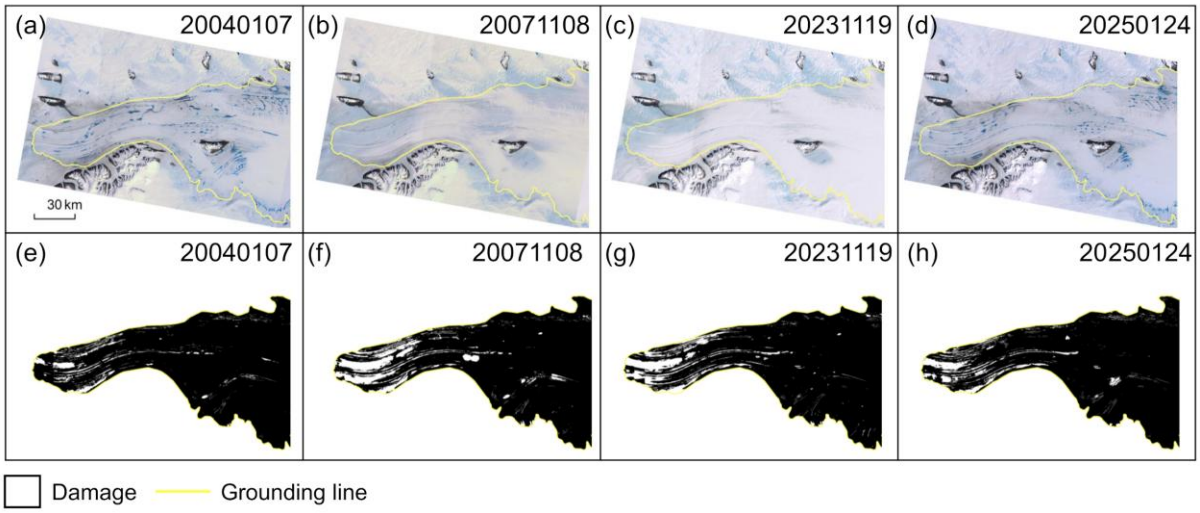


Figure S11. Representative images of the Amery Ice Shelf near the southern grounding line and their corresponding damage maps.

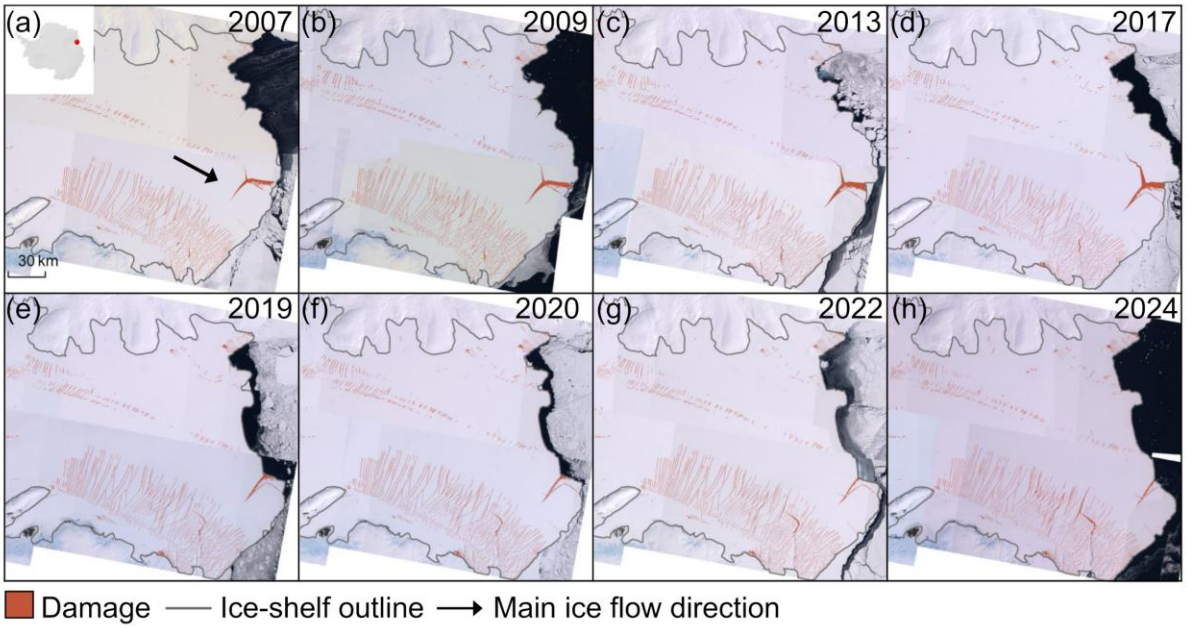


Figure S12. Representative surface damage maps of the front part of Amery Ice Shelf for (a) 2007, (b) 2009, (c) 2013, (d) 2017, (e) 2019, (f) 2020, (g) 2022 and (h) 2024. The location of Amery Ice Shelf in Antarctica is shown in (a).

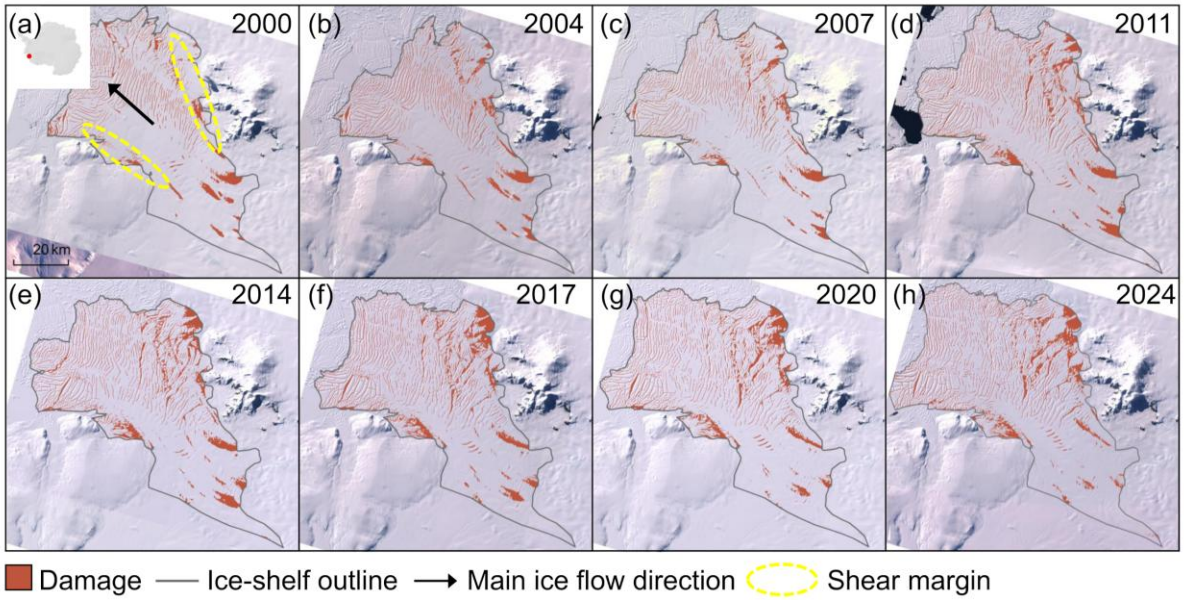


Figure S13. Representative surface damage maps of Crosson Ice Shelf for (a) 2000, (b) 2004, (c) 2007, (d) 2011, (e) 2014, (f) 2017, (g) 2020 and (h) 2024. The location of Crosson Ice Shelf in Antarctica is shown in (a).

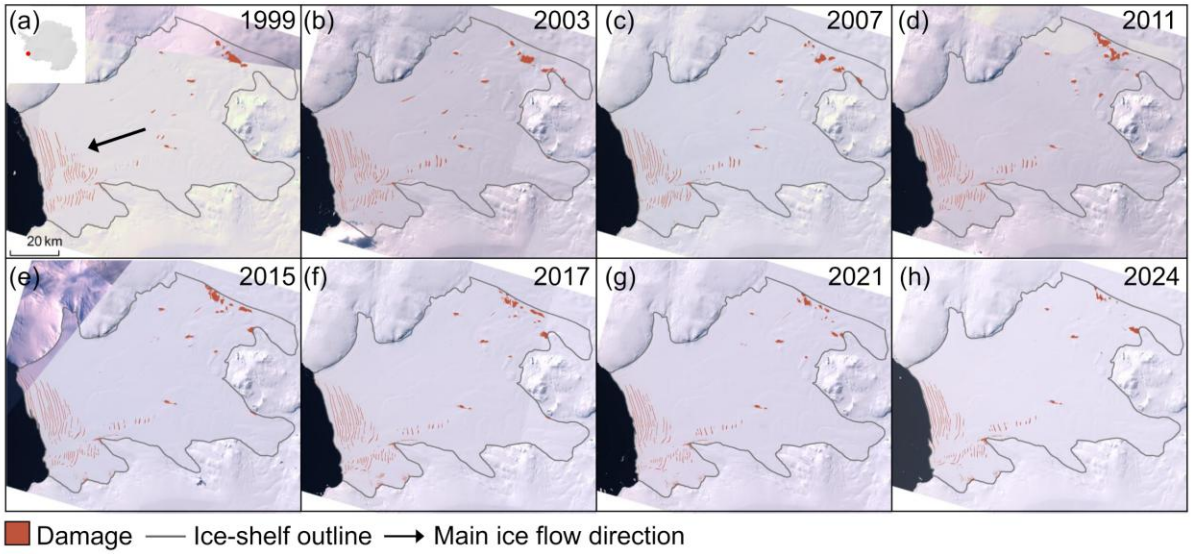


Figure S14. Representative surface damage maps of Dotson Ice Shelf for (a) 1999, (b) 2003, (c) 2007, (d) 2011, (e) 2015, (f) 2017, (g) 2021 and (h) 2024. The location of Dotson Ice Shelf in Antarctica is shown in (a).

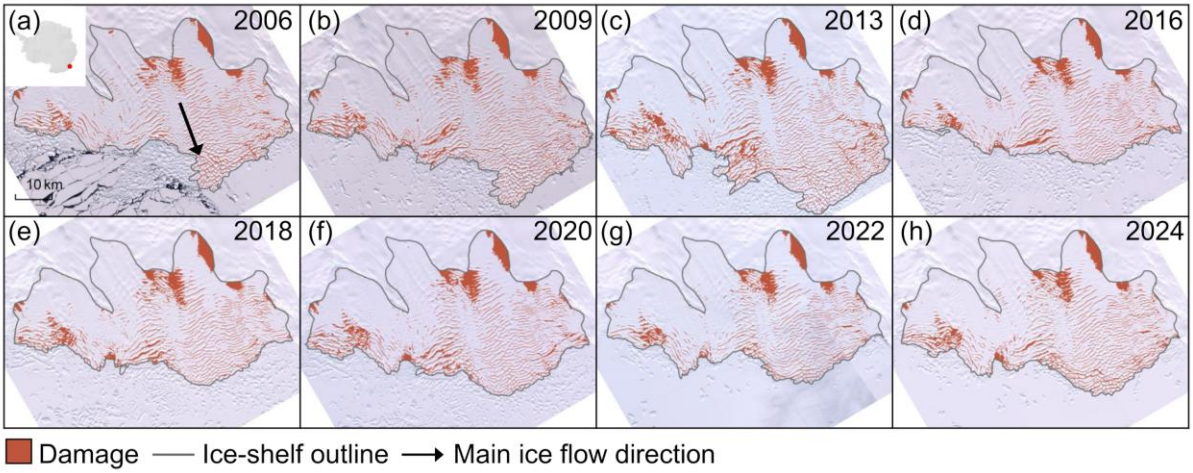


Figure S15. Representative surface damage maps of Holmes Ice Shelf for (a) 2006, (b) 2009, (c) 2013, (d) 2016, (e) 2018, (f) 2020, (g) 2022 and (h) 2024. The location of Holmes Ice Shelf in Antarctica is shown in (a).

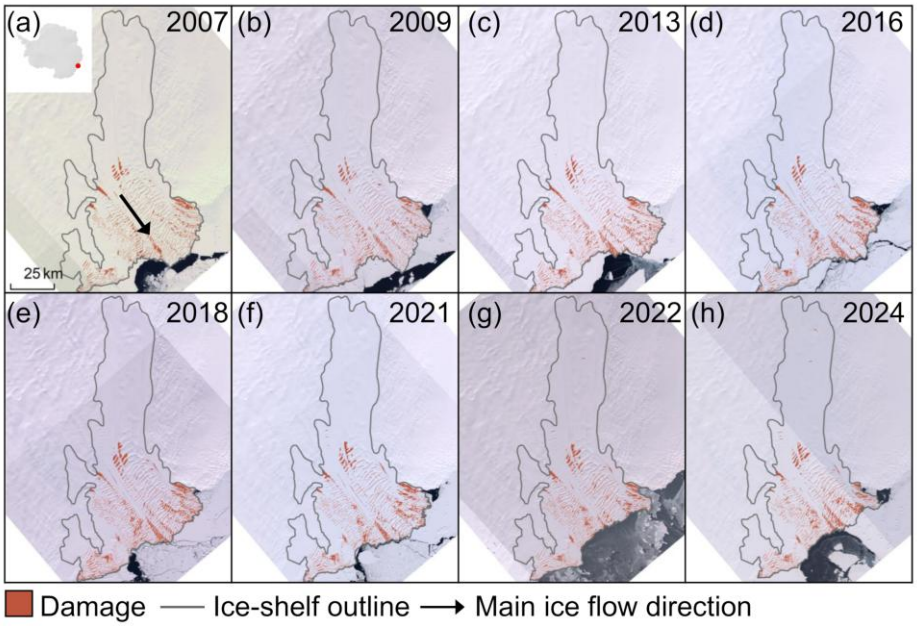


Figure S16. Representative surface damage maps of Totten Ice Shelf for (a) 2007, (b) 2009, (c) 2013, (d) 2016, (e) 2018, (f) 2021, (g) 2022 and (h) 2024. The location of Totten Ice Shelf in Antarctica is shown in (a).

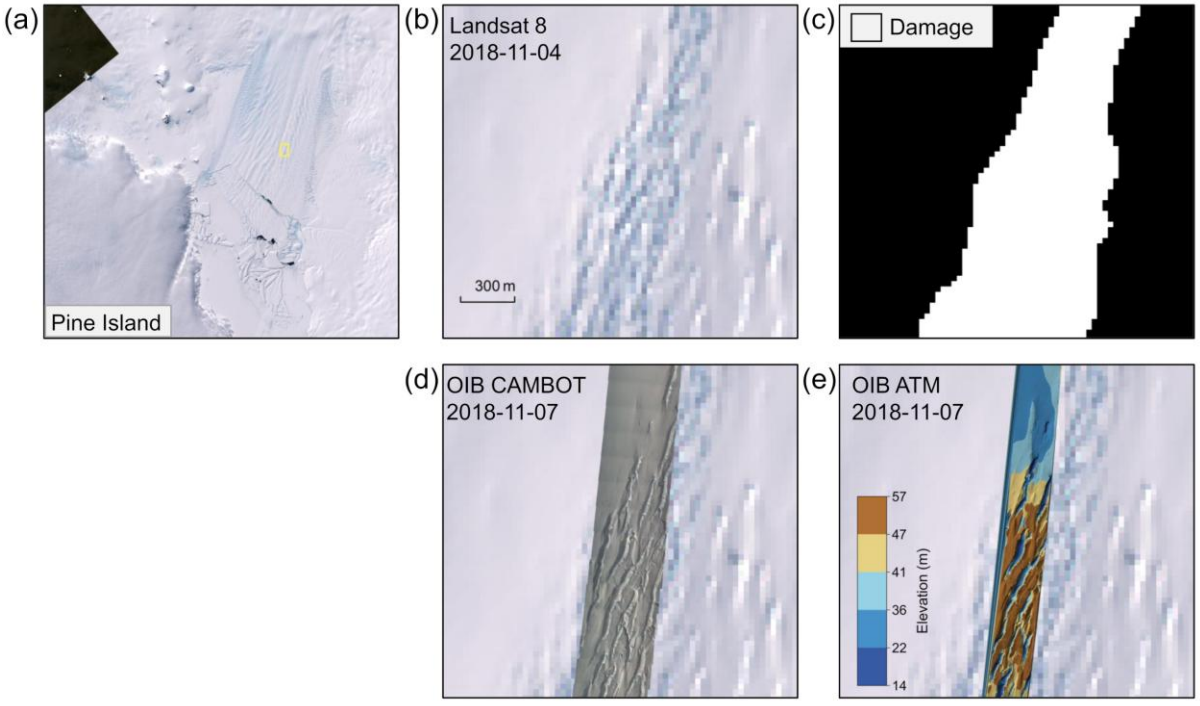


Figure S17. Comparison of damage characteristics across different data sources. (a) Landsat 8 RGB imagery of Pine Island Ice Shelf acquired on 2018-11-04, with the yellow box indicating the region shown in (b)–(e). (b) Enlarged view of the yellow-boxed region in (a). (c) Damage prediction for (b). (d) Operation IceBridge (OIB) CAMBOT L1B Geolocated Images acquired on 2018-11-07 and overlaid on (b). (e) Triangulated irregular network (TIN) generated from OIB ATM L1B elevation data acquired on 2018-11-07 and overlaid on (b).